ARTICLES

Is Møller–Plesset perturbation theory a convergent *ab initio* method?

Matthew L. Leininger,[a] Wesley D. Allen, and Henry F. Schaefer III
Center for Computational Quantum Chemistry, University of Georgia, Athens, Georgia 30602-2556

C. David Sherrill
School of Chemistry and Biochemistry, Georgia Institute of Technology, Atlanta, Georgia 30332-0400

(Received 7 February 2000; accepted 9 March 2000)

Recent studies have seriously questioned the use of higher-order Møller–Plesset perturbation theory (MP*n*) in describing electron correlation in atomic and molecular systems. Here we first reinvestigate with improved numerical techniques previously controversial and disturbing MP*n* energetic series for Ne, F^-, HF, BH, C_2 and N_2. Conspicuously absent in previous work is research on the convergence of MP*n* spectroscopic constants, and thus complete MP*n* (energy, r_e, ω_e) series were then computed for (BH, HF, CN^+, C_2 and N_2) through the high orders (MP25, MP21, MP13, MP39 and MP19) within the correlation consistent family of basis sets. A persistent, slowly decaying ringing pattern in the C_2 energy series was tracked out to MP155. Finally, new energy series were generated and analyzed through MP167 for Cl^- and MP39 for Ar and HCl. The MP*n* energy and property series variously display rapid or slow convergence, monotonic or oscillatory decay, highly erratic or regular behavior, or early or late divergence, all depending on the chemical system or the choice of one-particle basis set. For oscillatory series the spectroscopic constants computed from low-order MP*n* methods are often more accurate, with respect to the full configuration interaction (FCI) limit, than those computed via high-order MP*n* theory. © *2000 American Institute of Physics.* [S0021-9606(00)30221-5]

I. INTRODUCTION

Møller–Plesset Perturbation Theory (MP*n*) has undoubtedly been the most popular electron correlation approach in use over the last two decades, as widely disseminated program packages execute thousands of such computations daily worldwide. Efficient electronic structure implementations of MP*n* theory through fourth order have been in place for some time, and beginning in 1990 explicit capabilities for performing MP5 computations on small molecules began to appear.[1,2] In 1995 Kucharski and Bartlett[3] reported a full MP6 scheme based on coupled-cluster iterations at the CCSDTQ level. Shortly thereafter, Cremer and He[4–8] published an impressive series of papers on the development, implementation, and application of an explicit MP6 method by traditional techniques.

The tacit assumption behind chemical applications of MP*n* theory is that the perturbation series is convergent, at least for systems dominated by a single electronic configuration. Early work on the quantitative assessment of this assumption for a few model systems was stimulated in the mid 1980s by the advent of large-scale full CI methods.[9–12] The conclusions appeared to be that under normal circumstances (single-reference systems near equilibrium) the series are convergent but the truncation errors cannot be anticipated to diminish below 1 mE_h until well after sixth order. In cases of stretched bond distances and/or large spin contamination, convergence was shown to be erratic, deceptive,[11] or protracted even past 50th order.[12] In 1996 Olsen and co-workers[13] discovered peculiar and disturbing MP*n* convergence behavior on some seemingly innocuous systems such as Ne, HF, and H_2O, namely, that augmentation of standard valence double-ζ basis sets with diffuse functions suddenly causes the perturbation series for these species to diverge! A subsequent analysis[14,15] of the Ne and HF cases in terms of degeneracies in the Hamiltonian H_0+zV within the unit circle of the complex plane ($|z|\leqslant 1$) implicated ''back door'' intruder states as the origin of the MP*n* divergence. Meanwhile, Dunning and collaborators[16–19] have continued to execute systematic studies of molecular energies and properties with the aim of determining intrinsic errors in low-order MP*n* methods at the complete one-particle basis set limit. The current status, indeed crisis, of MP*n* theory is nicely summarized in the abstract of their March 1998 paper[16] on spectroscopic constants of first-row diatomic molecules: ''The perturbation expansions are, in general, only slowly converging and, for HF, N_2, CO, and F_2, appear to be far from convergence at MP4. In fact, for HF, N_2, and CO, the errors in the calculated spectroscopic constants for the MP4 method are *larger* than those for the MP2 method (the only exception is D_e). The current study, combined with other recent studies, raises serious doubts about the use of Møller–Plesset perturbation theory to describe electron correlation effects in atomic and molecular calculations.''

[a]Present address: Sandia National Laboratories, Livermore, CA 94551-0969.

Among the implications of such concerns is a questioning of the continued use of expensive MP4 computations[20] in widely used, predictive thermochemical schemes such as G2 and G3 theory,[21,22] or various CBS models.[23]

In this paper, we report high-order MP*n* benchmark correlation treatments for the atoms Ne, F^-, Ar, and Cl^- and diatomics BH, HF, C_2, CN^+, N_2 and HCl within the correlation consistent family of basis sets. To ascertain the numerical stability of prior studies and to ensure the accuracy of new computations, we modified an existing FCI algorithm to carry out high-order MP*n* computations in 64- and 128-bit precision and in either an orthonormal or nonorthogonal vector space.[12] These computations are utilized to determine the effectiveness of MP*n* theory in converging to the FCI limit. Almost all other benchmarks of this kind have focused on the MP*n* energy series alone, an exception being the very recent investigations[15,24] of divergent MP*n* behavior for the electric dipole and quadrupole moments of hydrogen fluoride. The current study addresses this dearth of property information by computing and analyzing complete MP*n* energy, r_e, and ω_e series.

II. METHODS

Developments in CI methodology in the 1980s lead to the implementation of efficient algorithms for computing the product of the Hamiltonian matrix on a vector ($\boldsymbol{\sigma}=\mathbf{Hc}$).[25–38] A formalism based on $\boldsymbol{\sigma}$ for constructing *n*th-order energies (E_n^k) and wave functions ($|\psi_n^k\rangle$) of the *k*-th eigenstate within Rayleigh–Schrödinger perturbation theory results by casting the fundamental perturbation equations (for $n \geqslant 1$) into a many-particle basis of Slater determinants,

$$E_{n+1}^k = \langle \psi_0^k | H | \psi_n^k \rangle, \tag{1}$$

and

$$(H_0 - E_0)|\psi_n^k\rangle = \sum_{i=1}^{n} E_i^k |\psi_{n-i}^k\rangle + H_0|\psi_{n-1}^k\rangle - H|\psi_{n-1}^k\rangle. \tag{2}$$

From Eq. (1) the $(n+1)$-th order energy can be computed from the overlap of the zeroth-order wave function with the $\boldsymbol{\sigma}$ vector corresponding to multiplication of the FCI Hamiltonian matrix on $|\psi_n^k\rangle$.[12] Alternatively, the Wigner energy formulas[39,40] allow the $(2n)$-th and $(2n+1)$-th order energies to be computed from the same matrix-vector product, thereby allowing much higher orders of perturbation theory to be reached for the same storage requirements:

$$E_{2n}^k = \langle \psi_{n-1}^k | H | \psi_n^k \rangle - \langle \psi_{n-1}^k | H_0 | \psi_n^k \rangle - \sum_{i=1}^{n} \sum_{j=1}^{n-1} E_{2n-i-j}^k \langle \psi_i^k | \psi_j^k \rangle, \tag{3}$$

and

$$E_{2n+1}^k = \langle \psi_n^k | H | \psi_n^k \rangle - \langle \psi_n^k | H_0 | \psi_n^k \rangle - \sum_{i=1}^{n} \sum_{j=1}^{n} E_{2n+1-i-j}^k \langle \psi_i^k | \psi_j^k \rangle. \tag{4}$$

According to Eq. (2), generation of the *n*th-order wave function involves multiplication of $|\psi_{n-1}^k\rangle$ on the FCI matrix, a subsequent linear combination with $H_0|\psi_{n-1}^k\rangle$ and all lower-order wave functions, and a final operation with the resolvent matrix.[9,12,41] The resolvent matrix can be trivially computed if $\mathbf{H}_0$ is diagonal; otherwise the *n*th-order wave function can be obtained by solving directly or iteratively the linear system in Eq. (2).

In the simplest implementation, the Hamiltonian matrix employed in the above equations is the FCI matrix containing all possible excitations. However, the explicit multiplication of a vector onto the FCI matrix is not always necessary, at least for the early terms of the MP*n* series. To obtain $\boldsymbol{\sigma}_n = \mathbf{H}|\psi_{n-1}^k\rangle$ only the diagonal excitation blocks of the Hamiltonian matrix through level $(2n-2)$, and higher off-diagonal coupling blocks of the types $(2n-3,\ 2n-1)$, $(2n-2,\ 2n-1)$, and $(2n-2,\ 2n)$ are required. A specific example is multiplying the Hamiltonian matrix on the first-order wave function, $|\psi_1^k\rangle$. Since the triple (T) and quadruple (Q) excitations are absent in the first-order wave function, no matrix elements involving the T-T, T-Q, and Q-Q classes are required;

$$\mathbf{H}|\psi_1^k\rangle = \begin{bmatrix} \langle\Phi_0|H|\Phi_0\rangle & \langle\Phi_0|H|S\rangle & \langle\Phi_0|H|D\rangle \\ \langle S|H|\Phi_0\rangle & \langle S|H|S\rangle & \langle S|H|D\rangle \\ \langle D|H|\Phi_0\rangle & \langle D|H|S\rangle & \langle D|H|D\rangle \\ 0 & \langle T|H|S\rangle & \langle T|H|D\rangle \\ 0 & 0 & \langle Q|H|D\rangle \end{bmatrix} \begin{bmatrix} c_1^0 \\ c_1^S \\ c_1^D \end{bmatrix} = \begin{bmatrix} \sigma_2^0 \\ \sigma_2^S \\ \sigma_2^D \\ \sigma_2^T \\ \sigma_2^Q \end{bmatrix}. \tag{5}$$

III. COMPUTATIONAL DETAILS

The sundry MP*n* series generated in this study are summarized in Table I along with pertinent computational details. All computations involved the (singlet) ground electronic states of the species listed, and all the zeroth-order wave functions were constructed from canonical, closed-shell, restricted-Hartree–Fock orbitals. The basis sets employed belong to the standard cc-pVXZ and aug-cc-pVXZ correlation-consistent families,[42–44] which possess pure spherical-harmonic polarization manifolds. In addition to FCI and high-order MP*n* data, comparative results were also obtained with the CCSD, CCSD(T), and CCSDT methods,[45–51] as well as with truncated CI wave functions. In all correlation treatments, the core orbitals (but no virtual orbitals) were removed (frozen) from the active space. All computations were performed using the PSI package,[52] as linked with the determinant-based configuration interaction program DETCI.[53]

Spectroscopic constants (r_e and ω_e) for the various electronic structure methods were determined by first generating energies of at least 10^{-10} E_h accuracy at points uniformly

TABLE I. Summary of MP*n* computations.

Species	Basis set	Basis size	H-L gap[a]	Series order[b]	FCI space[c]	Pattern
Ne	aug-cc-pVDZ	23	1140	39	6 693 283	Late, oscillatory divergence
F^-	aug-cc-pVDZ	23	690	39	6 693 283	Early, oscillatory divergence
Ar	aug-cc-pVDZ	27	742	39	6 693 283	Early, monotonic convergence
Cl^-	aug-cc-pVDZ	27	476	167	6 693 283	Very late, oscillatory divergence
$BH(^1\Sigma^+)$	cc-pVDZ	19	404	25	6129	Early, monotonic convergence
	cc-pVTZ	44	397	25	208 065	Early, monotonic convergence
	cc-pVQZ	85	392	25	3 068 596	Early, monotonic convergence
	aug-cc-pVDZ	32	375	25	56 467	Early, monotonic convergence
	aug-cc-pVTZ	69	374	25	1 319 122	Early, monotonic convergence
	aug-cc-pVQZ	126	372	25	15 132 412	Early, monotonic convergence
N_2	cc-pVDZ	28	763	19	540 924 024	Delayed, oscillatory convergence
$C_2(^1\Sigma_g^+)$	cc-pVDZ	28	342	155	27 944 940	Protracted, decaying ringing
$CN^+(^1\Sigma^+)$	cc-pVDZ	28	380	13	55 883 796	Early, oscillatory divergence
HF	cc-pVDZ	19	812	35	2 342 800	Erratic, early convergence
	aug-cc-pVDZ	32	686	21	247 513 357	Late, oscillatory divergence
HCl	aug-cc-pVDZ	36	615	39	247 513 357	Monotonic, early convergence

[a]HOMO-LUMO gap (mE_h) in canonical RHF orbitals.
[b]Highest term generated in the computations.
[c]Number of determinants. The computations for (Ne, F^-, Ar, Cl^-, N_2, C_2) and (BH, CN^+, HF, HCl) were performed in D_{2h} and C_{2v} symmetry, respectively.

distributed in 0.01 Å intervals about the best available bond distance. For each MP*n* or comparative level of theory, the five points which best enveloped the corresponding equilibrium bond distance were fit to a fifth-order polynomial under a simple constraint on the quintic force constant, as in earlier work.[54] Each fifth-order polynomial was then used to determine a precise value for r_e, the quadratic force constant at this point, and hence ω_e.

IV. RESULTS AND DISCUSSION

Here we reinvestigate the previous findings of Olsen *et al.*[13] and then discuss the convergence of the MP*n* ener-

TABLE II. MP*n* and comparative results for $X\ ^1\Sigma^+$ BH given by cc-pVXZ basis sets.

	cc-pVDZ			cc-pVTZ			cc-pVQZ		
	$\epsilon(mE_h)$[a]	r_e(Å)	$\omega_e(\mathrm{cm}^{-1})$	$\epsilon(mE_h)$[a]	r_e(Å)	$\omega_e(\mathrm{cm}^{-1})$	$\epsilon(mE_h)$[a]	r_e(Å)	$\omega_e(\mathrm{cm}^{-1})$
RHF	90.137	1.235 96	2492.6	101.231	1.222 06	2483.1	104.282	1.220 30	2487.3
MP2	29.414	1.246 74	2421.8	27.706	1.226 80	2431.1	26.133	1.224 75	2437.2
MP3	11.579	1.251 86	2384.8	11.144	1.231 30	2393.0	11.019	1.229 28	2399.9
MP4	5.227	1.254 99	2357.6	5.163	1.234 67	2363.5	5.148	1.232 65	2370.9
MP5	2.572	1.256 46	2343.3	2.619	1.236 05	2350.4	2.641	1.233 96	2358.4
MP6	1.316	1.256 92	2337.6	1.386	1.236 48	2345.3	1.407	1.234 38	2353.4
MP7	0.677	1.256 92	2336.3	0.748	1.236 48	2344.2	0.766	1.234 38	2352.3
MP8	0.343	1.256 75	2336.8	0.404	1.236 33	2344.6	0.419	1.234 23	2352.7
MP9	0.168	1.256 55	2337.7	0.217	1.236 16	2345.5	0.228	1.234 05	2353.6
MP10	0.077	1.256 37	2338.7	0.115	1.236 00	2346.4	0.123	1.233 89	2354.5
MP11	0.033	1.256 24	2339.4	0.060	1.235 88	2347.1	0.065	1.233 77	2355.2
MP12	0.011	1.256 14	2339.9	0.030	1.235 78	2347.7	0.034	1.233 67	2355.7
MP13	0.002	1.256 07	2340.3	0.015	1.235 72	2348.0	0.017	1.233 61	2356.1
MP14	−0.001	1.256 03	2340.5	0.007	1.235 67	2348.3	0.008	1.233 56	2356.4
MP15	−0.002	1.256 00	2340.6	0.003	1.235 64	2348.5	0.004	1.233 53	2356.5
MP16	−0.002	1.255 99	2340.6	0.001	1.235 63	2348.6	0.002	1.233 51	2356.6
MP17	−0.001	1.255 98	2340.7	0.000	1.235 61	2348.6	0.001	1.233 50	2356.7
MP18	−0.001	1.255 97	2340.7	0.000	1.235 61	2348.7	0.000	1.233 49	2356.7
MP19	−0.001	1.255 97	2340.7	0.000	1.235 60	2348.7	0.000	1.233 49	2356.7
MP20	0.000	1.255 97	2340.7	0.000	1.235 60	2348.7	0.000	1.233 49	2356.7
MP21-MP25	0.000	1.255 97	2340.7	0.000	1.235 60	2348.7	0.000	1.233 49	2356.8
CISD	4.467	1.253 45	2362.1	5.488	1.233 22	2372.0	5.711	1.231 14	2380.0
CISDT	2.739	1.254 59	2353.0	3.129	1.234 37	2361.7	3.208	1.232 34	2369.3
CCSD	1.853	1.254 80	2350.7	2.557	1.234 35	2360.5	2.720	1.232 19	2369.2
CCSD(T)	0.483	1.255 78	2342.6	0.521	1.235 40	2350.8	0.504	1.233 29	2358.9
CCSDT	0.067	1.256 03	2340.2	0.086	1.235 57	2348.9	0.089	1.233 46	2357.0
FCI	b	1.255 97	2340.7	b	1.235 60	2348.7	b	1.233 49	2356.8

[a]Error with respect to full CI energy at the full CI optimized geometry.
[b]The cc-pVDZ, cc-pVTZ, and cc-pVQZ FCI total energies are −25.215 324, −25.231 136, and −25.235 568 E_h, respectively.

TABLE III. MP*n* and comparative results for $X\,^1\Sigma^+$ BH given by aug- cc-pVXZ basis sets.

	aug-cc-pVDZ			aug-cc-pVTZ			aug-cc-pVQZ		
	$\epsilon(mE_h)$[a]	r_e(Å)	ω_e(cm^{-1})	$\epsilon(mE_h)$[a]	r_e(Å)	ω_e(cm^{-1})	$\epsilon(mE_h)$[a]	r_e(Å)	ω_e(cm^{-1})
RHF	92.163	1.232 79	2480.0	101.841	1.221 28	2485.4	104.483	1.220 08	2488.4
MP2	29.622	1.243 47	2404.6	27.439	1.226 71	2428.9	25.846	1.224 79	2436.2
MP3	11.654	1.249 02	2361.9	11.105	1.231 27	2390.6	11.023	1.229 29	2399.0
MP4	5.242	1.252 32	2334.0	5.171	1.234 65	2361.4	5.162	1.232 66	2370.1
MP5	2.566	1.253 85	2319.9	2.633	1.236 06	2348.2	2.651	1.234 00	2357.4
MP6	1.307	1.254 34	2314.4	1.397	1.236 51	2343.1	1.413	1.234 43	2352.3
MP7	0.673	1.254 36	2313.1	0.756	1.236 51	2341.9	0.770	1.234 43	2351.2
MP8	0.343	1.254 21	2313.6	0.410	1.236 37	2342.3	0.422	1.234 28	2351.7
MP9	0.171	1.254 02	2314.5	0.222	1.236 19	2343.2	0.230	1.234 10	2352.5
MP10	0.082	1.253 86	2315.4	0.118	1.236 03	2344.1	0.125	1.233 94	2353.4
MP11	0.036	1.253 73	2316.1	0.062	1.235 91	2344.9	0.066	1.233 82	2354.2
MP12	0.015	1.253 63	2316.7	0.032	1.235 81	2345.4	0.035	1.233 72	2354.7
MP13	0.005	1.253 57	2317.0	0.016	1.235 75	2345.8	0.018	1.233 66	2355.1
MP14	0.000	1.253 53	2317.2	0.007	1.235 70	2346.0	0.009	1.233 61	2355.3
MP15	−0.001	1.253 50	2317.4	0.003	1.235 67	2346.2	0.004	1.233 58	2355.5
MP16	−0.001	1.253 49	2317.4	0.001	1.235 65	2346.3	0.002	1.233 56	2355.6
MP17	−0.001	1.253 48	2317.5	0.000	1.235 64	2346.4	0.001	1.233 55	2355.7
MP18	−0.001	1.253 47	2317.5	0.000	1.235 64	2346.4	0.000	1.233 54	2355.7
MP19	−0.001	1.253 47	2317.5	0.000	1.235 63	2346.4	0.000	1.233 54	2355.7
MP20-MP25	0.000	1.253 47	2317.5	0.000	1.235 63	2346.4	0.000	1.233 53	2355.7
CISD	4.771	1.250 49	2342.4	5.578	1.233 10	2370.8	5.733	1.231 13	2379.5
CISDT	2.849	1.251 92	2331.4	3.148	1.234 37	2359.7	3.210	1.232 37	2368.4
CCSD	2.058	1.251 96	2329.6	2.631	1.234 24	2359.2	2.740	1.232 19	2368.5
CCSD(T)	0.529	1.253 14	2320.3	0.532	1.235 39	2348.8	0.501	1.233 33	2357.9
CCSDT	0.078	1.253 47	2317.4	0.089	1.235 59	2346.7	0.090	1.233 50	2356.0
FCI	b	1.253 47	2317.5	b	1.235 63	2346.4	b	1.233 53	2355.7

[a]Error with respect to full CI energy at full CI optimized geometry.
[b]The aug-cc-pVDZ, aug-cc-pVTZ, and aug-cc-pVQZ FCI total energies are −25.218 432, −25.232 012, and −25.235 843 E_h, respectively.

gies, equilibrium geometries, and harmonic vibrational frequencies for each molecule separately. A qualitative summary of the series and their patterns is given in Table I.

A. Olsen data

The species for which MP*n* energy series were reported by Olsen and co-workers[13] can be divided into three sets. In the set containing highly electronegative atoms (Ne, F^-, HF, H_2O), convergent series were found with the cc-pVDZ basis set, but oscillatory, divergent series were encountered upon augmentation with diffuse functions. In contrast, the (CH_2, BH) set displayed monotonic convergence for all basis sets employed. Finally, the (C_2, N_2) set showed irregular series patterns, with convergence in the former case still heavily in question at MP31. The divergent and irregular patterns in these results have been somewhat controversial and might be criticized as being numerical artifacts rather than physical effects. This criticism stems from the repeated matrix-vector products, linear dependence issues among the wave functions for the various orders, and the required cancellation of unlinked terms involved in generating the MP*n* series by FCI schemes. Nevertheless, in our reinvestigation the Olsen data were universally reproduced to the reported $10^{-6}\,E_h$ by our completely independent program DETCI.[53] The energies produced with the $n+1$ formula [Eq. (1)] matched those from the Wigner $(2n,\ 2n+1)$ formulas [Eqs. (3) and (4)] to within $10^{-13}\,E_h$. The computed energies were also stable to $10^{-13}\,E_h$ with respect to an increase in precision from 64- to

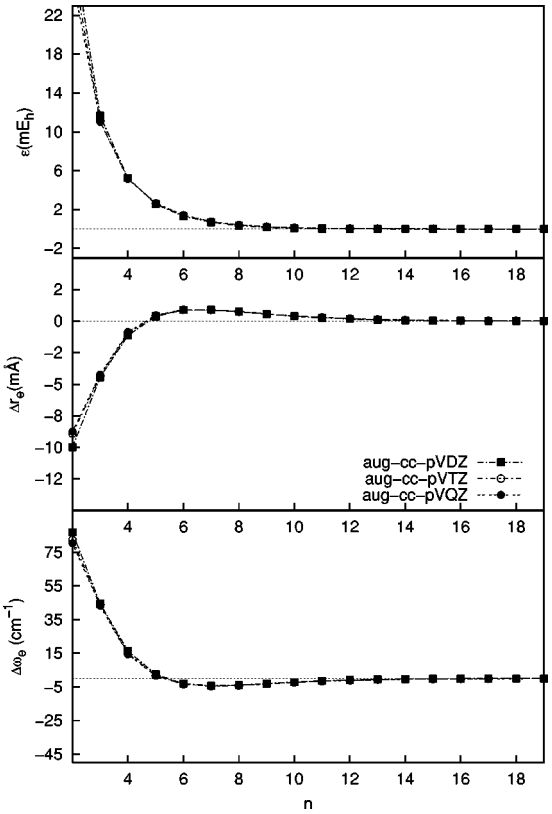

FIG. 1. Convergence behavior of MP*n* series toward FCI limits for $X\,^1\Sigma^+$ BH.

TABLE IV. MP*n* and comparative results for $X\ ^1\Sigma^+$ HF.

	cc-pVDZ			aug-cc-pVDZ		
	$\epsilon(mE_h)$[a]	r_e(Å)	$\omega_e(\mathrm{cm}^{-1})$	$\epsilon(mE_h)$[a]	r_e(Å)	$\omega_e(\mathrm{cm}^{-1})$
RHF	209.374	0.901 49	4440.7	231.083	0.900 18	4467.3
MP2	7.606	0.919 64	4169.9	8.372	0.924 81	4082.4
MP3	4.721	0.916 52	4218.2	7.760	0.919 37	4169.1
MP4	0.496	0.919 71	4157.1	−0.882	0.925 43	4056.4
MP5	0.435	0.919 66	4157.3	1.715	0.922 66	4111.0
MP6	−0.007	0.920 23	4144.7	−0.994	0.925 94	4043.1
MP7	0.072	0.920 10	4147.1	0.903	0.923 11	4104.4
MP8	−0.013	0.920 28	4142.9	−0.733	0.925 93	4040.4
MP9	0.014	0.920 21	4144.5	0.660	0.923 21	4104.9
MP10	−0.005	0.920 26	4143.0	−0.604	0.925 95	4037.2
MP11	0.004	0.920 23	4143.8	0.575	0.923 15	4108.9
MP12	−0.002	0.920 25	4143.2	−0.562	0.926 08	4031.0
MP13	0.001	0.920 24	4143.6	0.563	0.922 97	4116.5
MP14	−0.001	0.920 25	4143.3	−0.576	0.926 35	4020.7
MP15	0.001	0.920 24	4143.5	0.600	0.922 65	4128.5
MP16	0.000	0.920 25	4143.4	−0.636	0.926 79	4004.5
MP17	0.000	0.920 25	4143.5	0.684	0.922 16	4146.8
MP18	0.000	0.920 25	4143.4	−0.746	0.927 47	3979.1
MP19	0.000	0.920 25	4143.5	0.823	0.921 44	4174.2
MP20	0.000	0.920 25	4143.4	−0.917	0.928 52	3939.2
MP21	0.000	0.920 25	4143.5	1.033	0.920 37	4215.2
MP22-MP39	0.000	0.920 25	4143.4			
CISD	8.864	0.916 61	4209.2	12.506	0.919 14	4166.5
CISDT	7.031	0.917 42	4192.5	8.716	0.920 69	4137.5
CISDTQ	0.195	0.920 13	4145.7	0.380	0.924 28	4077.1
CISDTQP	0.087	0.920 19	4144.6	0.113	0.924 47	4073.6
CISDTQPH	0.002	0.920 25	4143.6	0.004	0.924 55	4072.2
CCSD	2.423	0.918 95	4169.0	4.707	0.922 19	4116.4
CCSD(T)	0.496	0.919 89	4150.1	0.536	0.924 10	4080.7
CCSDT	0.406	0.919 95	4148.5	0.335	0.924 26	4077.2
FCI	b	0.920 25	4143.5	b	0.924 56	4072.2

[a]Error with respect to full CI energy at the full CI optimized geometry.
[b]The cc-pVDZ and aug-cc-pVDZ FCI total energies are −100.228 652 and −100.264 177 E_h, respectively.

128-bit arithmetic and whether the expansion employed an orthonormal vector space or unaltered *n*th-order wave functions.[10,12] Therefore, numerical concerns appear to be unfounded. Our results, along with the determination of $H_0 + zV$ degeneracies for the Ne and HF cases,[14,15] demonstrate that the peculiar MP*n* phenomena[13] are real effects, not merely numerical errors.

B. $X\ ^1\Sigma^+$ BH

The results for $X\ ^1\Sigma^+$ BH in the standard and augmented (diffuse) correlation-consistent basis sets through quadruple-ζ and MP25 are presented in Tables II–III and Fig. 1. In the terminology of Cremer, ground-state BH is a ''class A'' system,[4] for which the MP*n* energy series essentially converges monotonically to the FCI limit. The rate of energy convergence is relatively rapid and strikingly unaffected by changes in the one-particle basis. While the r_e and ω_e series display similar, smooth convergence, both slightly overshoot the FCI asymptote around fifth order before settling into monotonic decay. The MP*n* convergence for all BH series is slow vis-à-vis coupled cluster methods, however; for example, with the aug-cc-pVQZ basis, the remarkable CCSD(T) (0.5 mE_h, 0.0002 Å, 2.2 cm^{-1}) and CCSDT (0.09 mE_h, 0.000 03 Å, 0.3 cm^{-1}) accuracies for (ε, r_e, ω_e) are not reached until (MP8, MP11, MP10) and (MP11, MP16, MP15), respectively.

C. $X\ ^1\Sigma^+$ HF

In Table IV and Fig. 2, data are presented for the hydrogen fluoride MP*n* energy, r_e, and ω_e series for the standard and diffuse cc-pVDZ basis sets. In the cc-pVDZ basis set the MP*n* energy error diminishes to 7 μE_h at MP6, rebounds to 72 μE_h at MP7, and finally dips below 5 μE_h at MP11. For r_e and ω_e, there are anomalous jumps to maximum errors at MP3 before similar, erratic decay to the FCI asymptotes. In stark contrast, augmenting the one-particle basis set with diffuse functions causes all three MP*n* series to oscillate and ultimately diverge. It is notable that the aug-cc-pVDZ property series blow up more rapidly than the energy series, as the amplitudes of the (r_e, ω_e) oscillations start increasing past (MP9, MP7), as compared to MP12 for ε. In either basis the molecular properties computed from the MP2 method are within (0.0007 Å, 27 cm^{-1}) of the FCI limit, and for aug-cc-pVDZ the MP*n* geometry and harmonic vibrational frequency predictions only deteriorate by including perturbative corrections beyond second order. The coupled-cluster meth-

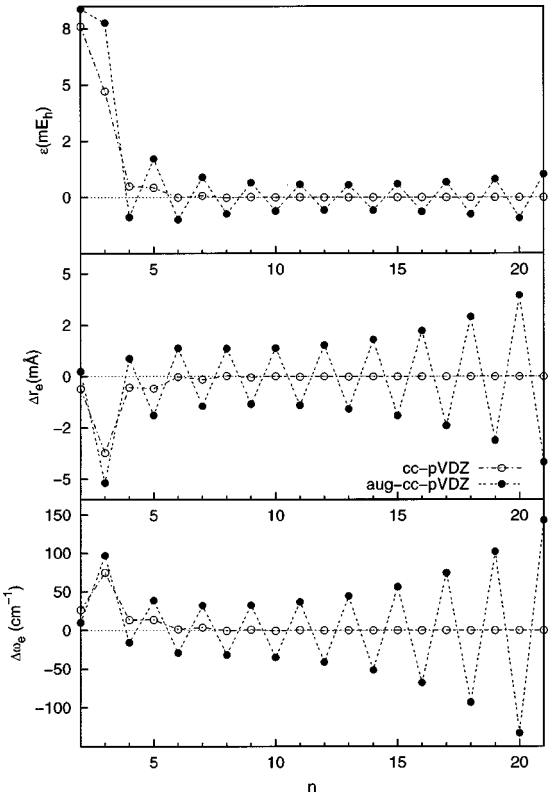

FIG. 2. Convergence behavior of MP*n* series toward FCI limits for $X\ ^1\Sigma^+$ HF.

TABLE V. MP*n* and comparative results for X $^1\Sigma^+$ CN^+.

	cc-pVDZ		
	$\epsilon(mE_h)$[a]	r_e(Å)	ω_e(cm^{-1})
RHF	380.477	1.159 10	2175.8
MP2	24.979	1.225 29	2342.2
MP3	84.109	1.185 34	2217.2
MP4	−21.910	1.235 29	1991.9
MP5	61.007	1.180 16	2224.7
MP6	−49.739	1.234 00	1667.1
MP7	78.723	1.166 98	2139.2
MP8	−95.674	c	c
MP9	132.176	1.130 20	2194.8
MP10	−174.891	c	c
MP11	231.916	1.072 54	2782.8
MP12	−304.645	c	c
MP13	393.148	1.021 34	3538.4
CISD	73.165	1.190 55	2099.4
CISDT	50.864	1.181 58	2071.0
CISDTQ	7.962	1.194 26	2005.4
CISDTQP	2.462	1.195 58	1995.7
CISDTQPH	0.162	1.197 74	1980.6
CCSD	33.193	1.194 67	2033.1
CCSD(T)	−0.231	1.183 36	1936.3
CCSDT	3.290	1.196 27	1993.6
FCI	b	1.197 88	1979.8

[a]Error with respect to full CI energy at the full CI optimized geometry.
[b]The FCI total energy is –91.997 969 E_h.
[c]$X\ ^1\Sigma^+$ CN^+ is unbound at this level of theory.

ods clearly provide better approaches for property predictions, as exemplified by the outperformance of MP5 by CCSD(T) in residual (r_e, ω_e) errors, roughly by factors of 2 and 4 in the cc-pVDZ and aug-cc-pVDZ cases, respectively. Nonetheless, in the favorable (convergent) cc-pVDZ MP*n* case, all predictions past fifth order exceed the accuracy of their CCSD(T) and CCSDT counterparts.

D. $X\ ^1\Sigma^+$ CN^+

The MP*n* series for CN^+ in a cc-pVDZ basis are reported in Table V and plotted in Fig. 3. This species exhibits an intricate electronic structure with a near degeneracy of the HOMO (4σ) and LUMO (5σ). A proper zeroth-order description of the electronic ground state should incorporate the $[(4\sigma)^2 \rightarrow (5\sigma)^2]$ pair excitation, which contributes almost 10% to the FCI wave function and whose attendant diradical character yields $\mathcal{T}_1$ diagnostics three times larger than the recommended single-reference cutoff.[55,56] Hence, single-reference Møller–Plesset perturbation theory is expected to have difficulties describing this molecular system. Figure 3 reveals that the energy and property series are strongly oscillatory and rapidly divergent, the differences between successive (ε, r_e, ω_e) terms never diminishing below (59 mE_h, 0.04 Å , 125 cm^{-1}). In fact, the oscillations become so wild that past MP7 the molecule dissociates in even orders and contracts to unphysically short distances in odd orders! For the low orders, the accuracy sequence is MP3>MP5>MP2>MP4 for r_e but MP4>MP3>MP5>MP2 for ω_e, illustrating the lack of a

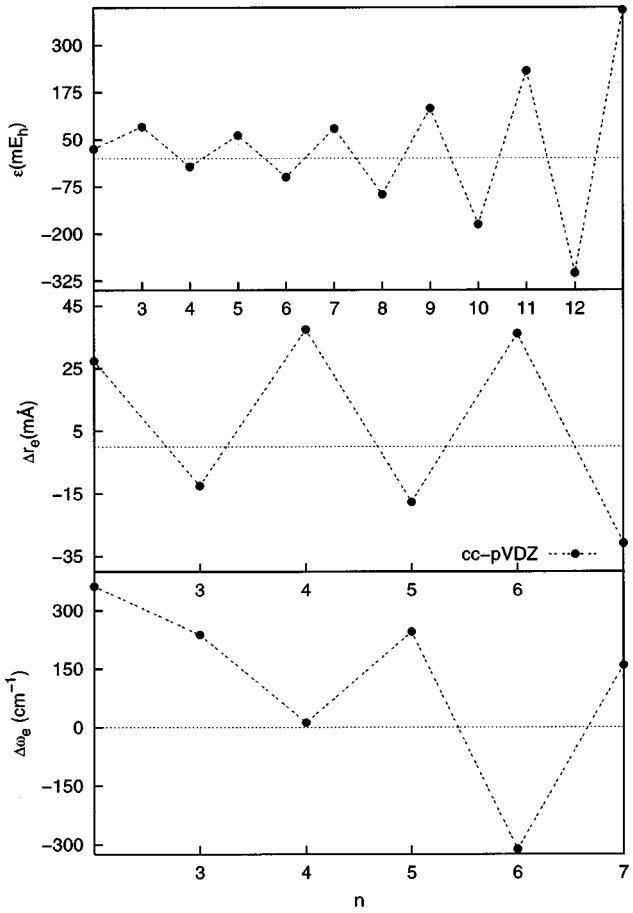

FIG. 3. Convergence behavior of MP*n* series toward FCI limits for $X\ ^1\Sigma^+$ CN^+.

TABLE VI. MP*n* and comparative results for X $^1\Sigma_g^+$ C_2.

	cc-pVDZ		
	$\epsilon(mE_h)$[a]	r_e(Å)	$\omega_e(\mathrm{cm}^{-1})$
RHF	343.396	1.252 33	1914.3
MP2	30.436	1.276 50	1873.0
MP3	65.094	1.251 40	1940.2
MP4	−8.062	1.295 42	1735.8
MP5	32.126	1.244 75	2023.3
MP6	−10.329	1.306 91	1584.5
MP7	17.839	1.243 87	2099.0
MP8	−7.577	1.313 92	1394.6
MP9	8.440	1.249 46	2115.2
MP10	−3.454	1.305 35	1317.2
MP11	2.074	1.259 30	2061.4
MP12	0.225	1.282 64	1537.8
MP13	−1.713	1.271 70	1934.1
MP14	2.487	1.266 19	1817.2
MP15	−3.262	1.285 50	1724.2
MP16	3.115	1.259 22	2005.1
MP17	−3.094	1.299 20	1411.5
MP18	2.444	1.258 80	2091.8
MP19	−1.903	1.305 54	1056.0
MP20	1.102	1.262 68	2087.0
MP21	−0.410	1.287 21	1317.7
MP22	−0.260	1.269 53	1995.9
MP23	0.796	1.271 46	1714.0
MP24	−1.163	1.278 54	1811.5
MP25	1.386	1.264 26	1956.3
MP26	−1.409	1.289 17	1504.0
MP27	1.313	1.262 49	2077.5
MP28	−1.071	1.299 84	991.7
MP29	0.767	1.264 30	2101.5
MP30	−0.406	1.289 20	1106.0
MP31	0.055	1.268 68	2037.4
MP32	0.269	1.274 30	1609.9
MP33	−0.527	1.275 06	1882.0
MP34	0.704	1.267 28	1902.6
MP35	−0.790	1.283 15	1604.8
MP36	0.784	1.264 92	2052.8
MP37	−0.700	1.292 96	1100.7
MP38	0.548	1.265 60	2102.6
MP39	−0.357	1.291 48	830.6
CISD	65.798	1.260 65	1897.2
CISDT	46.477	1.262 46	1884.6
CISDTQ	7.072	1.268 28	1841.0
CISDTQP	2.397	1.270 75	1827.0
CISDTQPH	0.144	1.272 73	1812.9
CCSD	29.957	1.266 16	1861.5
CCSD(T)	2.042	1.270 45	1828.1
CCSDT	3.371	1.270 73	1828.9
FCI	b	1.272 73	1812.9

[a]Error with respect to full CI energy at the full CI optimized geometry.
[b]The FCI total energy is −75.729 853 E_h.

consistent level of perturbation theory for error cancellation. Problems with perturbative approaches are also evident in the (T) correction, which induces a 0.01 Å change to the CCSD r_e value as opposed to the 0.0016 Å elongation of the full iterative triples (CCSDT). Similar results were report for CN^+ and BN in an earlier study by Watts and Bartlett.[57]

E. $X\ ^1\Sigma_g^+$ C_2

The C_2 molecule is isoelectronic with CN^+ and therefore presents similar problems for single-reference electronic structure methods. The $[(2\sigma_u)^2 \rightarrow (3\sigma_g)^2]$ pair excitation is equally important in the FCI wave function, but the $\mathcal{T}_1$ diagnostics are less than twice the single-reference standard.[55,56] In brief, deficiencies in MP*n* theory are not expected to be as pronounced as in the CN^+ case, and C_2 happens to be a system tantalizingly close to the convergence/divergence threshold. The cc-pVDZ MP*n* data for C_2 are shown in Table VI and Fig. 4. The energy series displays extended oscillations with amplitudes that very slowly damp out. The error with respect to the FCI energy never exceeds 3.5 mE_h past MP9, but it persists above 0.05 mE_h even past MP100. In essence, a fascinating pattern of protracted, decaying ringing with a period of about 10 is observed in the cc-pVDZ MP*n* series. Similar structure is observed in the property series, but the severity of the oscillations is of greater consequence. The r_e periodicity results in minimum errors of only (0.0038, −0.0010, −0.0013, 0.0016) Å at (MP2, MP13, MP23, MP32) but considerable maximum errors of (0.0412, 0.0328, 0.0271, 0.0202) Å at (MP8, MP19, MP28, MP37). Likewise, the ω_e periodicity spawns minimum errors of (60, 4, −1, 69) cm^{-1} at (MP2, MP14, MP24, MP33) but prodigious maximum errors of (−496, −757, −821, −982) cm^{-1} at (MP10, MP19, MP28, MP39). The maximum MP*n* property errors past ninth order, particular in ω_e, exhibit a striking lack of convergence, even though $|\varepsilon| < 3.5$ mE_h. The

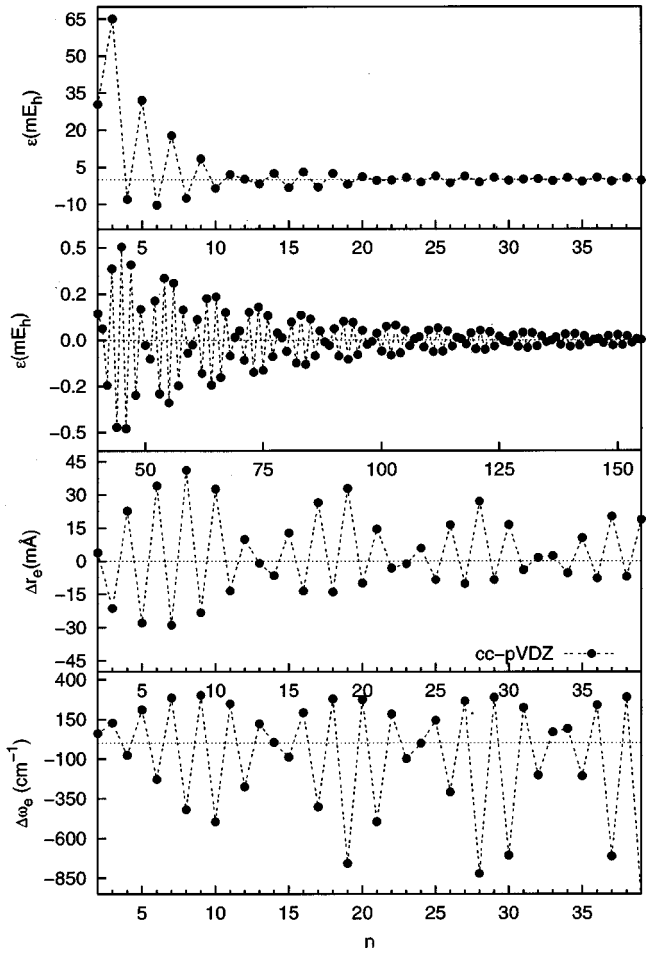

FIG. 4. Convergence behavior of MP*n* series toward FCI limits for $X\ ^1\Sigma_g^+$ C_2.

TABLE VII. MP*n* and comparative results for X $^1\Sigma_g^+$ N_2.

	cc-pVDZ		
	$\epsilon(mE_h)$[a]	r_e(Å)	ω_e(cm^{-1})
RHF	328.783	1.077 30	2757.6
MP2	15.606	1.129 87	2173.3
MP3	22.841	1.105 10	2529.4
MP4	−2.221	1.127 15	2199.1
MP5	3.953	1.114 55	2423.6
MP6	−0.550	1.122 23	2275.6
MP7	0.707	1.118 64	2356.3
MP8	−0.005	1.120 40	2314.8
MP9	0.085	1.119 94	2328.1
MP10	0.046	1.120 03	2325.7
MP11	−0.003	1.120 17	2321.8
MP12	0.021	1.120 05	2325.9
MP13	−0.004	1.120 16	2322.2
MP14	0.005	1.120 11	2324.5
MP15	−0.001	1.120 14	2323.2
MP16	0.000	1.120 13	2323.6
MP17	0.000	1.120 13	2323.5
MP18	0.000	1.120 13	2323.4
MP19	0.000	1.120 13	2323.5
CISD	36.402	1.104 96	2496.1
CISDT	25.903	1.108 66	2457.9
CISDTQ	2.300	1.118 20	2349.7
CISDTQP	0.797	1.119 45	2333.1
CISDTQPH	0.046	1.120 08	2324.3
CCSD	14.442	1.112 82	2408.8
CCSD(T)	1.862	1.118 93	2339.0
CCSDT	1.834	1.118 48	2346.6
FCI	b	1.120 13	2323.5

[a]Error with respect to full CI energy at the full CI optimized geometry.
[b]The FCI total energy is −109.278 340 E_h.

high orders of perturbation theory do not *converge* on (r_e, ω_e) values improved over MP2 (1.2765 Å, 1873 cm^{-1}) relative to FCI (1.2727 Å, 1813 cm^{-1}) until well after MP50. The reason for the incredible disparity in ω_e vs ε convergence becomes evident when the energy series of C_2 is generated out to MP155 for elongated bond distances. The ringing pattern of ε in Fig. 4 is retained for $r>1.30$ Å, but the oscillations become increasingly larger past MP50, indicating an onset of divergence in the [1.30, 1.31] Å interval. This onset of divergence only about 0.03 Å past the FCI r_e distance anomalously affects the curvatures of the high-order MP*n* curves, engendering the rather wild ω_e oscillations in Fig. 4. Once again, the coupled-cluster methods display entirely different behavior. To wit, while the CCSD(T) and CCSDT energy errors are commensurate with those past MP9, the robust, nonerratic character of these methods provides (r_e, ω_e) predictions to within (−0.0023 Å, 15 cm^{-1}) and (−0.0020 Å, 16 cm^{-1}) of the FCI values, respectively.

F. $X\ ^1\Sigma_g^+$ N_2

The MP*n* series for N_2 in a cc-pVDZ basis set through 19th order are shown in Table VII and Fig. 5. This molecule is seen to be a prototypical ''class B'' system,[4] for which the MP*n* energy series is oscillatory, but regular and convergent. The N_2 energy reaches 1 mE_h accuracy at MP6 and the 1 μE_h mark at MP15, lagging behind the convergence rate in the hydrogen fluoride case in the same basis set. The oscillatory property series both display an accuracy sequence of

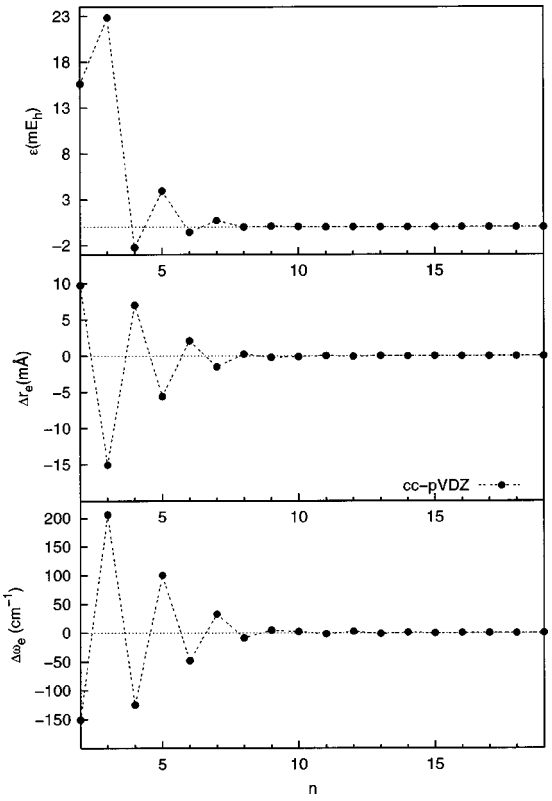

FIG. 5. Convergence behavior of MP*n* series toward FCI limits for $X\ ^1\Sigma_g^+$ N_2.

MP3<MP2<MP4<MP5, yet the FCI values are only reproduced to (0.006 Å, 100 cm^{-1}) at 5th order. Corrections beyond MP6 are necessary to reach the accuracy of CCSD(T) (0.0012 Å, 16 cm^{-1}) and CCSDT (0.0016 Å, 23 cm^{-1}).

G. $X\ ^1S$ Ar and Cl^-

As confirmed above, the aug-cc-pVDZ MP*n* energy series for ground-state Ne and F^- are divergent.[13,14] Here the isovalent species $X\ ^1S$ Ar and $X\ ^1S$ Cl^- are considered in the same basis set. The MP*n* energy data are shown in Table VIII and Fig. 6, and Fig. 7 provides a comparison to the Ne and F^- cases. In contrast to neon, the argon series exhibits exemplary, monotonic convergence to the FCI limit, with MP10 already yielding better than 1 μE_h accuracy and MP6 outperforming both CCSD(T) and CCSDT. In contrast, the Cl^- series manifests oscillatory divergence, but on a *much* weaker scale than for F^- (n.b.: the scales in Figs. 6 and 7 differ by more than two orders of magnitude). For Cl^- the closest approach to the FCI asymptote is 37 μE_h, occurring in the vicinity of MP24; however, the error increases only to 42 μE_h, at MP39. The deceptiveness of the series is demonstrated by the fact that (MP5, MP6) provides an energy closer to FCI than [CCSD(T), CCSDT]. Comparing the MP*n* behavior of (Ar, Cl^-) to (Ne, F^-), one is led to speculate that strong divergences might result from correlating the 2*s* and 2*p* core electrons in the former pair of atoms. Hence, for heavier atoms (beyond first row) the convergence of the MP*n* series might prove to be dependent on the frozen-core approximation.

TABLE VIII. MP*n* and comparative results for $X\ ^1S$ Ar, $X\ ^1S$ Cl^-, and $X\ ^1\Sigma^+$ HCl given by the aug-cc-pVDZ basis set.

	$X\ ^1S$ Ar $\epsilon(mE_h)$[a]	$X\ ^1S$ Cl^- $\epsilon(mE_h)$[a]	$X\ ^1\Sigma^+$ HCl $\epsilon(mE_h)$[a]
RHF	169.155	175.346	180.904
MP2	14.829	16.227	21.291
MP3	2.127	3.876	4.999
MP4	0.490	0.752	1.131
MP5	0.188	0.561	0.448
MP6	0.025	−0.051	0.086
MP7	0.015	0.148	0.052
MP8	0.002	−0.078	0.003
MP9	0.002	0.078	0.009
MP10	0.000	−0.063	−0.002
MP11	0.000	0.057	0.002
MP12	0.000	−0.051	−0.001
MP13	0.000	0.047	0.001
MP14	0.000	−0.044	−0.001
MP15	0.000	0.042	0.000
MP16	0.000	−0.040	0.000
MP17	0.000	0.039	0.000
MP18	0.000	−0.038	0.000
MP19	0.000	0.038	0.000
MP20	0.000	−0.037	0.000
MP21	0.000	0.037	0.000
MP22	0.000	−0.037	0.000
MP23	0.000	0.037	0.000
MP24	0.000	−0.037	0.000
MP25	0.000	0.037	0.000
MP26	0.000	−0.037	0.000
MP27	0.000	0.037	0.000
MP28	0.000	−0.038	0.000
MP29	0.000	0.038	0.000
MP30	0.000	−0.038	0.000
MP31	0.000	0.039	0.000
MP32	0.000	−0.039	0.000
MP33	0.000	0.040	0.000
MP34	0.000	−0.040	0.000
MP35	0.000	0.041	0.000
MP36	0.000	−0.041	0.000
MP37	0.000	0.041	0.000
MP38	0.000	−0.042	0.000
MP39	0.000	0.042	0.000
CISD	8.787	12.651	12.427
CISDT	6.229	8.647	8.415
CISDTQ	0.198	0.441	0.371
CISDTQP	0.063	0.127	0.113
CISDTQPH	0.001	0.004	0.003
CCSD	2.968	4.805	4.718
CCSD(T)	0.443	0.689	0.695
CCSDT	0.253	0.370	0.340
FCI	b	b	b

[a]Error with respect to full CI energy. $X\ ^1\Sigma^+$ HCl energies computed at r_e of 1.3124 Å .

[b]The $X\ ^1S$ Ar, $X\ ^1S$ Cl^-, and $X\ ^1\Sigma^+$ HCl FCI total energies are −526.970 128, −459.738 991, and −460.272 768 E_h .

H. $X\ ^1\Sigma^+$ HCl

The $X\ ^1\Sigma^+$ HCl MP*n* energy series in an augmented double-ζ basis is reported in Table VIII. The hydrogen chloride MP*n* aug-cc-pVDZ series does not display the same divergent behavior as that of the isovalent hydrogen fluoride, rather it converges quickly with (MP5, MP6) improving upon the [CCSD(T), CCSDT] results.

V. CONCLUSIONS

In summary, the convergence of the Møller–Plesset perturbation series has been assessed for several atoms and diatomic molecules exhibiting a range of electronic structures. A qualitative summary of the various series and their patterns are given in Table I. The computations of Olsen *et al.*[13] were confirmed within the reported μE_h accuracy, thus sup-

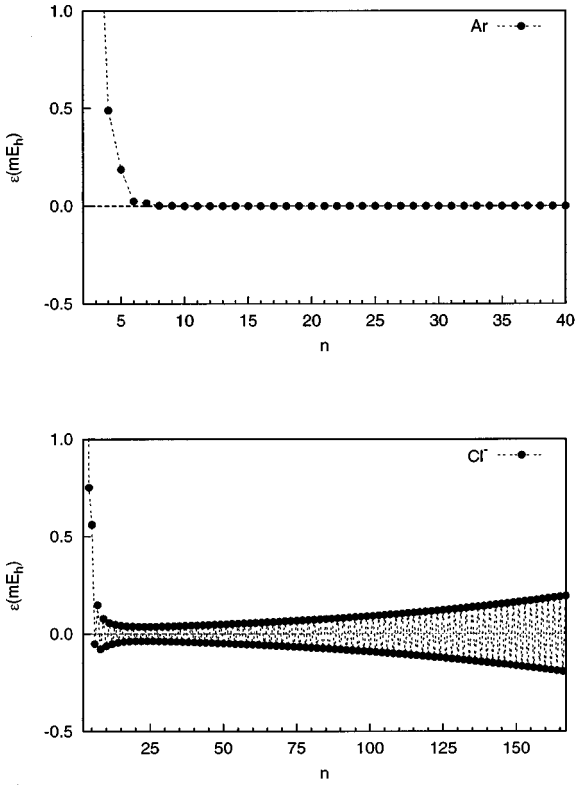

FIG. 6. Convergence behavior of aug-cc-pVDZ MP*n* energies toward FCI limits for $X\ ^1S$ Ar and $X\ ^1S$ Cl^-.

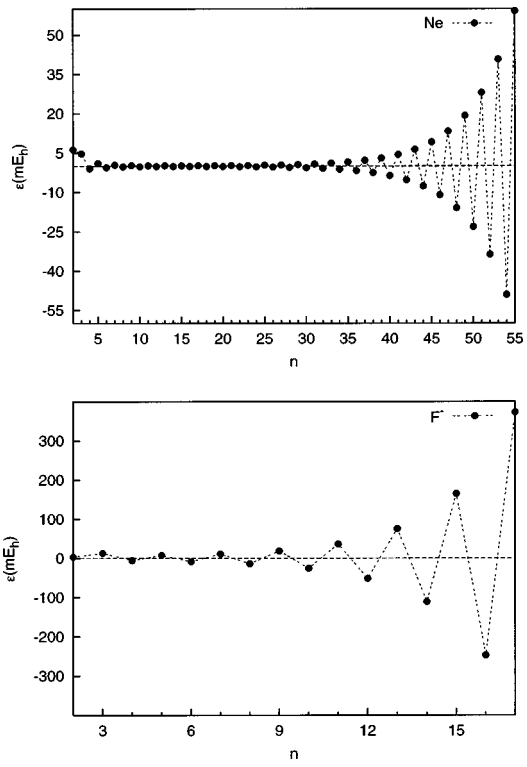

FIG. 7. Convergence behavior of aug-cc-pVDZ MP*n* energies toward FCI limits for $X\ ^1S$ Ne and $X\ ^1S$ F^-.

porting the fact that the peculiar MP*n* phenomena are physical effects, not merely numerical errors. The convergence of the MP*n* energy, r_e and ω_e series is strongly dependent on the chemical system and the one-particle basis set. The divergent behavior observed in diffuse basis sets appears to persist when larger, more balanced diffuse basis sets are used.[58] For the HF and C_2 molecules, higher-order perturbative corrections do little to improve upon the MP2 r_e and ω_e values. Various resummation techniques, such as Padé approximants and Feenberg scaling,[8,9,59–62] have the potential to extract a monotonically convergent perturbation series, and a quantitative assessment of their performance and reliability will be executed in a followup study. Similar to other recent MP*n* studies,[13–16,24] this work seriously questions the use of higher-order MP theory to account for electron correlation in atomic and molecular systems. Although computations involving higher-order Møller–Plesset theory can be utilized to elucidate the role of higher-order excitations in other many-body methods (e.g., coupled cluster), we recommend that extreme care be taken when employing higher-order MP*n* theory for chemical problems. In general it may be prudent to restrict the use of MP*n* theory to MP2 and use alternative coupled cluster methods to achieve a higher degree of accuracy.

ACKNOWLEDGMENTS

M.L.L. would like to thank Edward Valeev for many helpful discussions, Chris Barden for assistance with the $X\,^1\Sigma^+$ HCl data and Shawn Brown for assistance with the figures. This research was supported by the United States National Science Foundation, Grant No. CHE-9815397.

[1] K. Raghavachari, J. A. Pople, E. S. Replogle, and M. Head-Gordan, J. Phys. Chem. **94**, 5579 (1990).
[2] GAUSSIAN 94, Revision C.3, M. J. Frisch, G. W. Trucks, H. B. Schlegel, P. M. W. Gill, B. G. Johnson, M. A. Robb, J. R. Cheeseman, T. Keith, G. A. Petersson, J. A. Montgomery, K. Raghavachari, M. A. Al-Laham, V. G. Zakrzewski, J. V. Ortiz, J. B. Foresman, J. Cioslowski, B. B. Stefanov, A. Nanayakkara, M. Challacombe, C. Y. Peng, P. Y. Ayala, W. Chen, M. W. Wong, J. L. Andres, E. S. Replogle, R. Gomperts, R. L. Martin, D. J. Fox, J. S. Binkley, D. J. Defrees, J. Baker, J. P. Stewart, M. Head-Gordon, C. Gonzalez, and J. A. Pople (Gaussian, Inc., Pittsburg, PA, 1995).
[3] S. A. Kucharski and R. J. Bartlett, Chem. Phys. Lett. **237**, 264 (1993).
[4] D. Cremer and Z. He, J. Phys. Chem. **100**, 6173 (1996).
[5] Z. He and D. Cremer, Int. J. Quantum Chem. **59**, 15 (1996).
[6] Z. He and D. Cremer, Int. J. Quantum Chem. **59**, 31 (1996).
[7] Z. He and D. Cremer, Int. J. Quantum Chem. **59**, 57 (1996).
[8] Z. He and D. Cremer, Int. J. Quantum Chem. **59**, 71 (1996).
[9] W. D. Laidig, G. Fitzgerald, and R. J. Bartlett, Chem. Phys. Lett. **113**, 151 (1985).
[10] P. J. Knowles, K. Somasundram, N. C. Handy, and K. Hirao, Chem. Phys. Lett. **113**, 8 (1985).
[11] P. M. W. Gill and L. Radom, Chem. Phys. Lett. **132**, 16 (1986).
[12] N. C. Handy, P. J. Knowles, and K. Somasundram, Theor. Chim. Acta **68**, 87 (1985).
[13] J. Olsen, O. Christiansen, H. Koch, and P. Jørgensen, J. Chem. Phys. **105**, 5082 (1996).
[14] O. Christiansen, J. Olsen, P. Jørgensen, H. Koch, and P. A. Malmqvist, Chem. Phys. Lett. **261**, 369 (1996).
[15] H. Larsen, A. Halkier, J. Olsen, and P. Jørgensen, J. Chem. Phys. **112**, 1107 (2000).
[16] T. H. Dunning, Jr. and K. A. Peterson, J. Chem. Phys. **108**, 4761 (1998).
[17] K. A. Peterson and T. H. Dunning, Jr., J. Mol. Struct. **400**, 93 (1997).
[18] K. A. Peterson and T. H. Dunning, Jr., J. Phys. Chem. **99**, 3898 (1995).
[19] D. Feller and K. A. Peterson, J. Chem. Phys. **108**, 154 (1998).
[20] L. A. Curtiss, P. C. Redfern, K. Raghavachari, and J. A. Pople, Chem. Phys. Lett. **313**, 600 (1999).
[21] L. A. Curtiss, K. Raghavachari, G. W. Trucks, and J. A. Pople, J. Chem. Phys. **94**, 7221 (1991).
[22] L. A. Curtiss, K. Raghavachari, P. C. Redfern, V. Rassolov, and J. A. Pople, J. Chem. Phys. **109**, 7764 (1998).
[23] G. A. Petersson, in *Computational Thermochemistry, Prediction and Estimation of Molecular Thermodynamics*, edited by K. K. Irikura and D. J. Frurip (American Chemical Society, Washington, D. C., 1998), pp. 237–266.
[24] A. Halkier, H. Larsen, J. Olsen, and P. Jørgensen, J. Chem. Phys. **110**, 7127 (1999).
[25] I. Shavitt, Int. J. Quantum Chem., Symp. **11**, 131 (1977).
[26] I. Shavitt, Int. J. Quantum Chem., Symp. **12**, 5 (1978).
[27] B. R. Brooks and H. F. Schaefer, J. Chem. Phys. **70**, 5092 (1979).
[28] P. E. M. Siegbahn, J. Chem. Phys. **70**, 5391 (1979).
[29] N. C. Handy, Chem. Phys. Lett. **74**, 280 (1980).
[30] P. E. M. Siegbahn, J. Chem. Phys. **72**, 1647 (1980).
[31] P. Saxe, H. F. Schaefer, and N. C. Handy, Chem. Phys. Lett. **79**, 202 (1981).
[32] P. Saxe, D. J. Fox, H. F. Schaefer, and N. C. Handy, J. Chem. Phys. **77**, 5584 (1982).
[33] P. E. M. Siegbahn, Chem. Phys. Lett. **109**, 417 (1984).
[34] P. J. Knowles and N. C. Handy, Chem. Phys. Lett. **111**, 315 (1984).
[35] J. Olsen, B. O. Roos, P. Jørgensen, and H. J. Aa. Jensen, J. Chem. Phys. **89**, 2185 (1988).
[36] P. J. Knowles, Chem. Phys. Lett. **155**, 513 (1989).
[37] P. J. Knowles and N. C. Handy, J. Chem. Phys. **91**, 2396 (1989).
[38] R. J. Harrison and S. Zarrabian, Chem. Phys. Lett. **158**, 393 (1989).
[39] A. Dalgarno and A. L. Stewart, Proc. R. Soc. London, Ser. A **238**, 269 (1956).
[40] P. O. Löwdin, J. Math. Phys. **6**, 1341 (1965).
[41] A convenient way to incorporate the orthogonality of $|\psi_n^k\rangle$ to $|\psi_0^k\rangle$ and thus to completely define the *n*th-order wave function in the full configuration basis is to add a projection operator onto the zeroth-order space to the left side of Eq. (2), yielding a nonsingular resolvent operator $(H_0\text{-}E_0+|\psi_0^k\rangle\langle\psi_0^k|)^{-1}$.
[42] T. H. Dunning, Jr., J. Chem. Phys. **90**, 1007 (1989).
[43] R. A. Kendall, T. H. Dunning, Jr., and R. J. Harrison, J. Chem. Phys. **96**, 6796 (1992).
[44] D. E. Woon and T. H. Dunning, Jr., J. Chem. Phys. **98**, 1358 (1993).
[45] G. D. Purvis and R. J. Bartlett, J. Chem. Phys. **76**, 1910 (1982).
[46] G. E. Scuseria, C. L. Janssen, and H. F. Schaefer, J. Chem. Phys. **89**, 7382 (1988).
[47] K. Raghavachari, G. W. Trucks, J. A. Pople, and M. Head-Gordon, Chem. Phys. Lett. **157**, 479 (1989).
[48] R. J. Bartlett, J. Phys. Chem. **93**, 1697 (1989).
[49] Y. S. Lee, S. A. Kucharski, and R. J. Bartlett, J. Chem. Phys. **81**, 5906 (1984).
[50] G. E. Scuseria and H. F. Schaefer, Chem. Phys. Lett. **152**, 382 (1988).
[51] R. J. Bartlett, in *Modern Electronic Structure Theory, Vol. 1*, edited by D. R. Yarkony (World Scientific, Singapore, 1995).
[52] C. L. Janssen, E. T. Seidl, G. E. Scuseria, T. P. Hamilton, Y. Yamaguchi, R. B. Remington, Y. Xie, G. Vacek, C. D. Sherrill, T. D. Crawford, J. T. Fermann, W. D. Allen, B. R. Brooks, G. B. Fitzgerald, D. J. Fox, J. F. Gaw, N. C. Handy, W. D. Laidig, T. J. Lee, R. M. Pitzer, J. E. Rice, P. Saxe, A. C. Scheiner, and H. F. Schaefer, PSI 2.0.8 (PSITECH, Inc., Watkinsville, GA, 1995).
[53] C. D. Sherrill and H. F. Schaefer, in *Advances in Quantum Chemistry*, edited by P.-O. Löwdin (Academic, New York, 1999), Vol. 34, p. 143.
[54] M. L. Leininger, C. D. Sherrill, W. D. Allen, and H. F. Schaefer, J. Chem. Phys. **108**, 6717 (1998).
[55] T. J. Lee, J. E. Rice, G. E. Scuseria, and H. F. Schaefer, Theor. Chim. Acta **75**, 81 (1989).
[56] T. J. Lee and P. R. Taylor, Int. J. Quantum Chem., Symp. **23**, 199 (1989).
[57] J. D. Watts and R. J. Bartlett, Int. J. Quantum Chem. **28**, 195 (1994).
[58] J. Olsen, personal communication.
[59] E. Feenberg, Phys. Rev. **103**, 1116 (1956).
[60] B. Forsberg, Z. He, Y. He, and D. Cremer, Int. J. Quantum Chem. **76**, 306 (2000).
[61] R. J. Bartlett and I. Shavitt, Chem. Phys. Lett. **50**, 190 (1977).
[62] D. Z. Goodson, J. Chem. Phys. **112**, 4901 (2000).